Extended High-Gain Observer for Mars Entry Guidance

Kai Wu*[1], Hutao Cui[1], Pingyuan Cui[2]
[1]Deep Space Exploration Research Center, Harbin Institute of Technology, Harbin, China
[2]Deep Space Exploration Technology Institute, Beijing Institute of Technology, Beijing, China
*Corresponding author, e-mail:wkdf2003@gmail.com

Abstract

To deliver a Mars entry vehicle to the prescribed parachute deployment point, active entry guidance is essential. This paper addresses the problem of Mars atmospheric entry guidance through drag tracking method with extended high gain observer. First, an extended high gain observer combined with feedback linearization is applied in drag tracking for Mars entry longitudinal guidance. The observer estimates the drag and drag rate for drag tracking, estimates the perturbation due to model uncertainty and disturbance, and compensate for the perturbation by canceling its estimate. Then, bank reversal is adopted in the lateral plane to reduce the cross-range error. Finally, Mars entry simulation is performed to assess the performance of the adaptive guidance law. The results demonstrate that the proposed guidance law exhibits good performance.

Keywords: mars entry guidance, high gain observer, feedback linearization, Monte-Carlo

1. Introduction

In recent years, the concept of pinpoint landing has been proposed for Mars landing exploration missions to satisfy the scientific objectives and reduce risks of mission failure. Pinpoint landing requires the three-sigma position dispersion at the end of parachute deployment below approximately 3km, which is a large improvement upon former landing position uncertainties on the order of several hundred kilometers [1]. As demonstrated by Wolf [2]，the most efficient way to increase the landing accuracy is achieved during the atmospheric entry by guiding and controlling the vehicle trajectory in order to eliminate the dispersions caused at entry and accumulated during the hypersonic phase.

Many scholars have paid a lot of attention to Mars entry guidance [3-10]. And drag-based guidance methods have proven to be very effective in the Apollo and Shuttle programs [11,12], and were applied to Mars entry guidance research by many scholars [3-6]. Drag-based entry guidance strategy offers distinct advantages. On the one hand, various in-flight and terminal constraints imposed on the vehicle can be represented as drag constraints. On the other hand, Drag can be determined accurately from accelerometer measurements and the downrange to be flown by the vehicle can be determined exactly by the drag profile. So, the drag tracking approach can achieve the guidance requirements with robustness to modeling errors in atmospheric density and vehicle aerodynamics, which are main error sources [7, 8].

Feedback linearization (FL) used in ref. [4-6] to track drag can cancel nonlinearities and achieves asymptotic tracking under the idea conditions of no model uncertainty and disturbance. However the model uncertainty and disturbance exist in practice, which can introduce errors into FL control. And the FL control applied in Mars entry needs drag and drag rate information. While drag is determined directly, the drag rate needs to be computed either numerical differentiation or a model-based analytic expression, which also introduces errors into FL control. To recover the ideal performance of the FL control in presence of uncertainties and disturbance, this paper uses extended high-gain observer (EHGO) [13-15] to estimate drag rate and combined modeling error due to model uncertainty and disturbance which enables error compensation. The structure of this paper is as follows: Section 2 introduces the Mars entry equations used in this paper. Section 3 describes the new drag-based tracking longitudinal guidance method with extended high-gain observer. The bank reversal for lateral control is introduced in Section 4. In Section 5, simulation is performed and results are discussed. Finally, Section 6 gives the conclusion.

2. Three Degrees of Freedom Dynamic Equations

The Mars lander is modeled as an unpowered point mass flying in a stationary atmosphere of a nonrotating and spherical planet. The three degrees of freedom dynamic equations are

$$\dot{r} = V \sin \gamma \tag{1}$$

$$\dot{V} = -D - g \sin \gamma \tag{2}$$

$$\dot{\gamma} = L \cos \sigma / V + (V/r - g/V) \cos \gamma \tag{3}$$

$$\dot{\theta} = V \cos \gamma \sin \psi / r / \cos \lambda \tag{4}$$

$$\dot{\lambda} = V \cos \gamma \cos \psi / r \tag{5}$$

$$\dot{\psi} = V \sin \psi \cos \gamma \tan \lambda / r + L \sin \sigma / V / \cos \gamma \tag{6}$$

Where r is the distance from the center of the Mars to the mass center of the entry vehicle, V is the velocity of the entry vehicle, γ is the flight path angle, θ is the longitude, λ is the latitude, ψ is the heading angle defined as a clockwise rotation angle starting at due north, σ is the bank angle defined as the angle about the velocity vector from the local vertical plane to the lift vector. An inverse square gravitational acceleration $g = \mu/r^2$, where $\mu = GM_{mars}$ is assumed. L and D are the aerodynamic lift and drag accelerations, defined by

$$D = \rho V^2 S C_D / 2m, \ L = \rho V^2 S C_L / 2m \tag{7}$$

Where C_D and C_L are the aerodynamic drag and lift coefficients respectively, which are assumed to be constant, S is the vehicle reference surface area, m is the mass of the entry vehicle. ρ is the Mars atmospheric density, defined by the universal exponential density model

$$\rho = \rho_r \exp\left[(r_r - r)/h_s\right] \tag{8}$$

Where ρ_r is the density at the reference distance r_r, h_s is the constant scale height.
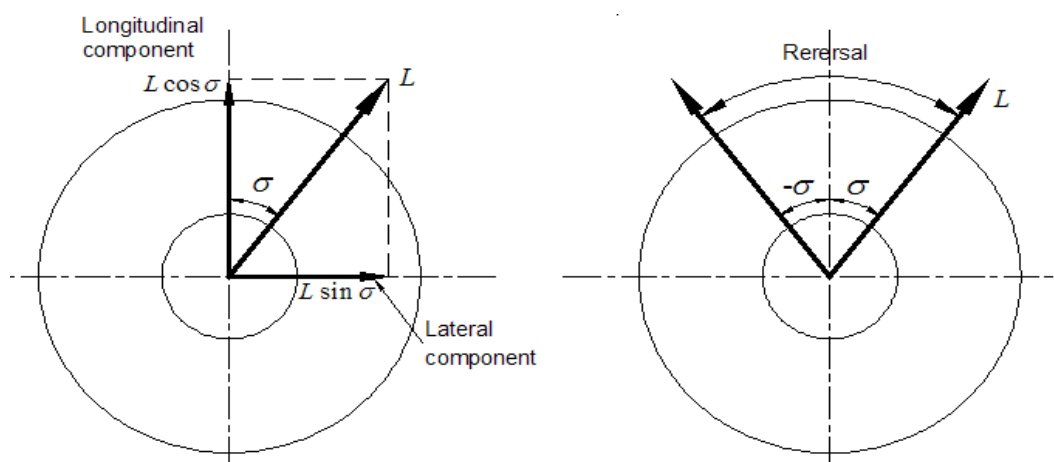
Figure 1. Effects of Selecting Different Switching Under Dynamic Condition

The vehicle's flight path is modified by rotating the lift vector around the axis formed by the velocity vector. The angle the lift vector is rotated is the bank angle, σ. Figure 1 shows the components of lift in the longitudinal and lateral planes. It is easy to see that a change of the sign of σ only affects the lateral motion, since $\sin(-\sigma) = -\sin(\sigma)$ but $\cos(-\sigma) = \cos(\sigma)$. This allows for the decoupling of the longitudinal dynamics and lateral dynamics provided that the Coriolis accelerations are small and the bank reversal is performed fast enough. So the longitudinal guidance can be solved changing the magnitude of σ, and the lateral guidance can be solved using bank reversals, which is a change of the sign of σ via a fast rotation of the lift vector.

3. Longitudinal Guidance Design

Firstly, defined the rang to go as the distance along the flight path to the target point, and is given by a drag-energy profile. The specific energy is defined as

$$E = V^2/2 + \left(\mu/R_{Mars} - \mu/R\right) \tag{9}$$

Differentiating E with respect to time yields

$$dE/dt = -VD \tag{10}$$

Then the predicted rang to go r_p is given by

$$r_p = \int_{V_f}^{V_c} V \, dt = \int_{E_c}^{E_f} dE/D \tag{11}$$

Where V_c and V_f are the current velocity, E_c and E_f are the current and terminal specific energies. Equation 11 implies that flying a specified drag-energy profile gives a specified down-range distance.

In longitudinal entry guidance, D is considered as the output of the longitudinal dynamic and $\cos\sigma$ as control input. We need to command the bank angle magnitude to track the reference drag. In order to construct the mathematical relationship between the output D and control input $\cos\sigma$, the drag needs to be twice Lie differentiated, because it has relative degree two. The result is as follows

$$\ddot{D} = b\left(V, \gamma, r, D, \dot{D}\right) + a\left(V, \gamma, D, \dot{D}\right)u \tag{12}$$

Where

$$b\left(V, \gamma, r, D, \dot{D}\right) = -\dot{D}\left(V\sin\gamma/h_s + 4D/V + 2g\sin\gamma/V\right) + D\sin\gamma/h_s\left(D + g\sin\gamma\right) - 2D/V^2\left(D + g\sin\gamma\right)^2$$
$$+ 4Dg\sin^2\gamma/r + D\cos^2\gamma/h_s\left(g - V^2/r\right) + 2Dg\cos^2\gamma/V^2\left(g - V^2/r\right)$$
$$a\left(V, \gamma, D, \dot{D}\right) = -DL\cos\gamma(2g/V^2 + 1/h_s)$$

Where control input $u \, \Box \, \cos\sigma$, and $\dot{D} = -DV\sin\gamma/h_s - 2D/V\left(D + g\sin\gamma\right)$

The longitudinal guidance law is to command the control input $u \, \Box \, \cos\sigma$ to track the reference drag profile and achieve the desired rang to go r_t at the same time during entry phase. It includes drag profile initialization, drag profile updating and drag tracking.

3.1. Drag Profile Initialization

The initial drag profile is programmed beforehand considering various in-flight and terminal constraints imposed on the vehicle. Then it is approximated by a Nth-order polynomial.

$$D_r(E) = \sum_{i=0}^{N} C_i E^i \tag{13}$$

Where C_i are polynomial fitting coefficients, E in Equation 13 is calculated by estimated velocity and altitude, which in turn provides the reference drag value D_r. $N = 6$ is considered to be suitable [4].

3.2. Drag Profile Updating
The reference drag profile is periodically updated to null the error between the predicted rang to go by

$$r_p = \int_{E_c}^{E_f} 1/D_r^{\text{up}}(E) dE \tag{14}$$

And the estimated distance to the target. Where $D_r^{\text{up}}(E) = [1 + \eta f(E)] D_r(E)$, The constant η is determined iteratively to null the range error. The shaping function $f(E)$ is given by

$$f(E) = 2\left(1 - \sqrt{2}\left(\varepsilon(E) - 0.5\right)^2\right) \tag{15}$$

Where $\varepsilon(E) = (E - E_c)/(E_f - E_c)$.

Then $D_r^{\text{up}}(E)$ is fit using the least squares approach according to the Equation 13, and replaces $D_r(E)$ in the drag reference generation for the next part of the trajectory.

3.3. Drag Tracking
Let $e = D - D_r$, then $\dot{e} = \dot{D} - \dot{D}_r$ and $\ddot{e} = \ddot{D} - \ddot{D}_r$. Using Equation 12, we obtain the drag error equation

$$\ddot{e} = b + au - \ddot{D}_r \tag{16}$$

Converting Equation 16 into the normal form [13] yields

$$\dot{x} = Ax + B\left(b + au - \ddot{D}_r\right) \tag{17}$$

$$y = Cx \tag{18}$$

Where $x = \begin{bmatrix} e & \dot{e} \end{bmatrix}^{\text{T}}$, the output $y = e = D - D_r$ $A = \begin{bmatrix} 0 & 1 \\ 0 & 0 \end{bmatrix}$, $B = \begin{bmatrix} 0 & 1 \end{bmatrix}^{\text{T}}$, $C = \begin{bmatrix} 1 & 0 \end{bmatrix}$.

The goal is to design an output feedback controller to asymptotically regulate the output y to zero, for all initial states in the compact set of interest, while meeting certain requirements on the transient response. If there are no uncertainties, no disturbance and no estimate errors, a and b in Equation 17 can be exactly known. Then FL which is often used in a lot of literature [4-6] can be used to cancels the nonlinear terms a and b of the drag dynamics and achieve exponential tracking. The FL tracking law is given by

$$u = \left(-b + \ddot{D}_r - Kx\right)/a \tag{19}$$

Where, $K = \begin{bmatrix} k_1 & k_2 \end{bmatrix}$ is chosen using a linear control design method to make $(A - BK)$ Hurwitz which means the origin of the closed-loop system is exponentially stable, and shape the transient response.

In practice, the external disturbance and uncertainties in atmospheric conditions and vehicle aerodynamics really exist and cannot be ignored. Moreover, navigation errors cannot be avoided and should be considered. In this case, the actual values of a and b are unknown, and it is only possible to calculate estimate values $\hat{a}$ and $\hat{b}$, which greatly degrades the performance of tracking law shown in Equation 19. So, extended high-gain observer (EHGO) is proposed to solve this problem. EHGO can estimate the combined modeling error and recover the ideal performance of the FL tracking in Equation 19 [14,15].

Defining the perturbation $\phi = b - \hat{b} + (a - \hat{a})u$, the EHGO is given by

$$\dot{\hat{x}} = A\hat{x} + B[\hat{\phi} + \hat{b} + \hat{a}u - \ddot{D}_r] + H(\varepsilon)(y - C\hat{x}) \tag{20}$$

$$\dot{\hat{\phi}} = (\alpha_{n+1}/\varepsilon^{n+1})(y - C\hat{x}) \tag{21}$$

Where $H(\varepsilon) = \left[\alpha_1/\varepsilon, ..., \alpha_n/\varepsilon^n\right]^{\mathrm{T}} \sqrt{a^2 + b^2}$, $\alpha_1, ..., \alpha_n, \alpha_{n+1}$ are chosen such that the polynomial $s^{n+1} + \alpha_1 s^n + ... + \alpha_{n+1}$ is Hurwitz, and $\varepsilon > 0$ is a small parameter. The control law is taken as

$$u = \left[-\hat{\sigma} - \hat{b}(\hat{\boldsymbol{x}}) + \ddot{D}_r - \boldsymbol{K}\hat{\boldsymbol{x}}\right] \big/ \hat{a}(\hat{\boldsymbol{x}}) \tag{22}$$

Where $\boldsymbol{K}$ is chosen to make $(A - \boldsymbol{BK})$ Hurwitz like Equation 19. However the transient response of the high-gain observer suffers from the peaking phenomenon. In addition to inducing unacceptable transient response, the peaking phenomenon could destabilize the closed-loop nonlinear system [14]. Fortunately, we can overcome the peaking phenomenon by saturating the control outside a compact region of interest to create a buffer that protects the states from peaking. Then the final output feedback controller is

$$u = \mathrm{sat}\left\{\left[-\hat{\sigma} - \hat{b}(\hat{\boldsymbol{x}}) + \ddot{D}_r - \boldsymbol{K}\hat{\boldsymbol{x}}\right] \big/ \hat{a}(\hat{\boldsymbol{x}})\right\} \tag{23}$$

Theorems 1 and 2 in [14] has concluded that the EHGO tracking system making up of Equation 20, Equation 21 and Equation 23 can recover the stability and transient performance of the nominal closed-loop system under feedback linearization. Performance recovery is achieved in the sense that the difference between the trajectory of the actual and nominal system can be made arbitrarily small by choosing the high gain observer parameter ε sufficiently small. Moreover, the EHGO can offer the estimation of $\dot{D}$ for drag tracking.

4. Lateral Guidance Design

Equation 6 represents the lateral dynamic. The lateral guidance is to switch the sign of σ to control the lateral motion and reduce cross-range error. A change of the sign of σ makes the vehicle turn to the opposite bank angle but leaves the longitudinal dynamics mostly unchanged. The swiching logic for commanding the sign of σ is based on a heading error corridor. The heading error is defined as the angle error between the local horizontal projection of the current azimuth and a line to the target. The maximum heading error is defined as a function of the range to the target r_t. The heading error corridor adopted here is shown in Figure 2. Once the heading error exceeds the specified tolerance, swiching the sign of σ is performed. It is should be noticed that bank reversal manoeuvres are not instantaneous in practice. An error in the propagation of the longitudinal trajectory with respect to the actual trajectory may be induced during the time interval required to perform a bank reversal. However, the lateral guidance is not the focus of this paper, and changing the sign of σ is considered to be fast enough in this paper. So, the error induced by bank reversal can be ignored.
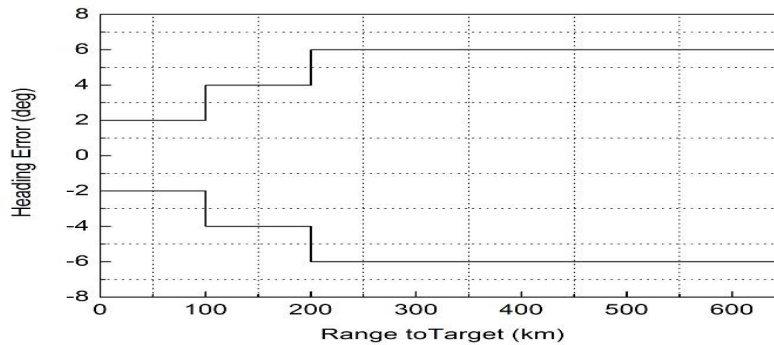
Figure 2. Heading Angle Error Corridor

5. Results and Analysis

In order to assessing the performance of the entry guidance method proposed in this paper, computer simulation and analysis in the MATLAB/Simulink environment has been carried out. The configuration and physical parameters of Mars Science Laboratory vehicle (MSL) [1] are used as an example to perform simulation and analysis in this paper. Vehicle mass m =2804kg, reference area S =15.9m^2, lift-to-drag ratio L/D =0.24, ballistic coefficient $\beta = m/C_D/S$ =120kg/m^2, Mars radius R_{Mars} =3397.2km, gravitational constant μ =42828.376212km^2/s^3, reference density ρ_r =0.00078kg/m3, reference distance r_0 =31.8km, scale height h_s =10km. The observer parameter α_1 =6, α_2 =11, α_3 =6, ε =0.1, and control parameter $K = \begin{bmatrix} k_1 & k_2 \end{bmatrix}$ =[0.4 0.04].

The system uncertainties considerd in this paper are separated into three parts: initial states uncertainties, aerodynamic uncertainties and atmospheric uncertainties, which are main error sources in Mars entry. The initial entry conditions and corresponding uncertainties are shown in Tabel 1. The uncertainties of vehicle aerodynamic and Mars atmospheric density are represented through changing the lift-to-drag ratio L/D and the reference density ρ_r, also shown in Tabel 1.

Table 1. Initial State Values and Uncertainties of Vehicle

Parameter	Mean value	Variation(3σ)	Type of uncertainty
Initial radial distance r_0 (km)	3457.2	1	Gaussian
Initial vehicle velocity V_0 (m/s)	5700	20	Gaussian
Initial flight path angle γ_0 (deg)	-14	0.1	Gaussian
Initial longitude θ_0 (deg)	0	0.05	Gaussian
Initial latitude λ_0 (deg)	0	0.05	Gaussian
Initial azimuth angle ψ_0 (deg)	0	0.1	Gaussian
Lift-to-drag ratio L/D	0.24	0.024	Gaussian
Ballistic coefficient β (kg/m^2)	120	12	Gaussian
Atmospheric density ρ_r (kg/m3)	0.00078	0.000117	Gaussian

5.1. Performance of EHGO

Firstly, the performance of the EHGO in estimating drag and drag rate is assessed in the present of various uncertainties. For the sake of simplicity, only longitudinal guidance is considered in this part. Figure 3 shows the drag and drag rate estimations of EHGO. The estimate curve and actual curve of drag are obviously different before 0.6s, but they are almost coincident after 0.6s. The estimate curve of drag rate behaves the same as the drag estimate. This indicates EHGO can accurately and enough fast estimate the drag and drag rate. Figure 4 shows the performance of EHGO+FL control. It can be found that the refence drag can be asymptotically tracked, and the final error approaches zero, which demonstrates that the

EHGO+FL tracking system can recover the ideal performance of the FL control in presence of uncertainties and disturbance.
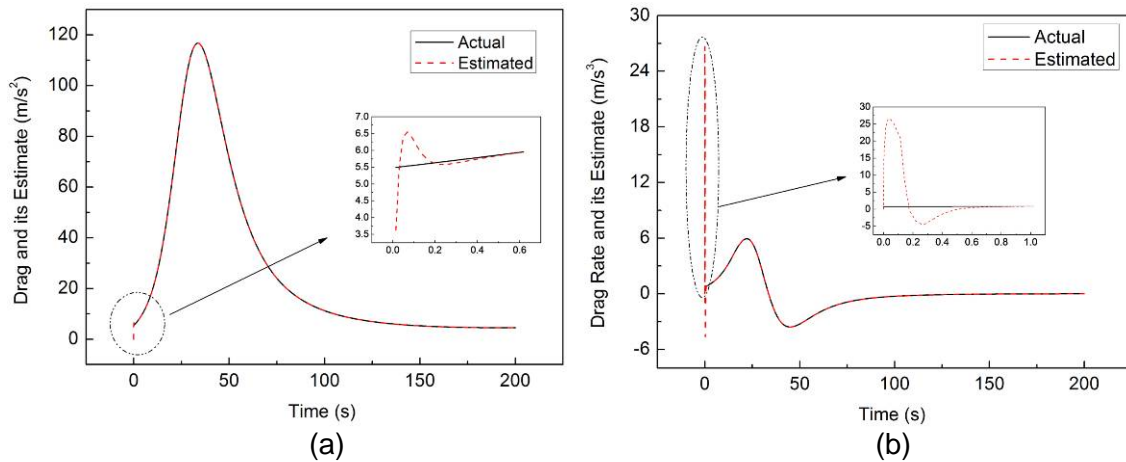
Figure 3. Drag and Drag Rate Estimates of EHGO (a) Drag and its Estimate (b) Drag Rate and its Estimate
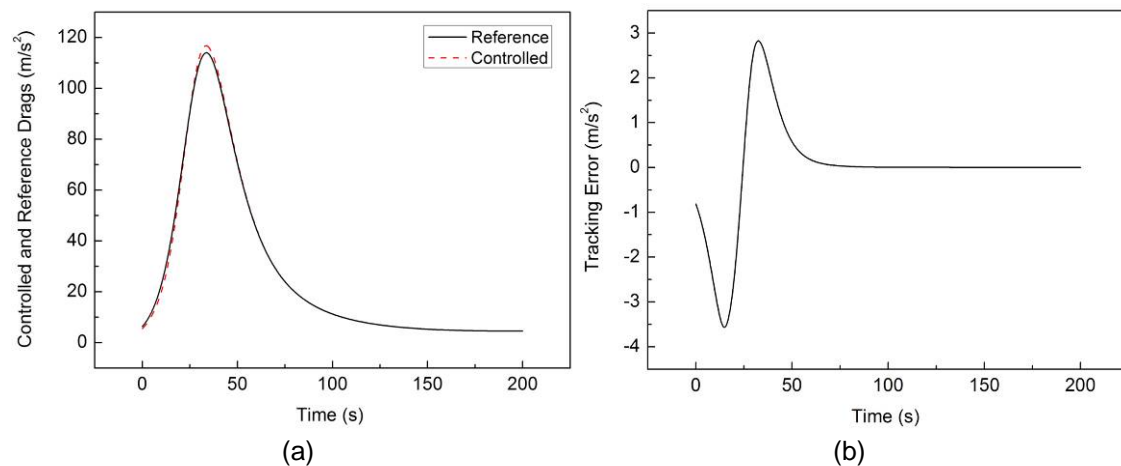
Figure 4. Performance of EHGO+FL Control (a) Reference and Controlled Drag (b) Tracking Error

5.2. Monte-Carlo Simulation of Mars Entry Guidance

Monte-Carlo analysis is a numerical technique often used to study systems with many coupled degrees of freedom that have significant uncertainty in their inputs and behavior. The technique utilizes known probability distributions of system inputs and parameters to generate probability distributions of the system output. To get a more accurate estimate of the response of a system, a large number of simulations with different combinations of these dispersed parameters must be conducted to determine the output of the system under various possible real world conditions. In order to further test the performance of EHGO+FL guidance method, a 2000-run Monte-Carlo simulation for both the EHGO+FL guidance and FL guidance with various uncertainties shown in Table 1 is carried out. Figure 5 shows the target miss distance dispersion of EHGO+FL guidance. The maximum longitudinal error and latitudinal error corresponding to the worst case are less than 8.6km, which can meet the requirement of future Mars pin-point landing exploration. Figure 6 shows the the target miss distance dispersion of FL guidance with

the same uncertainties. It can be found that the maximum error reaches 18km and is more the EHGO+FL control error.
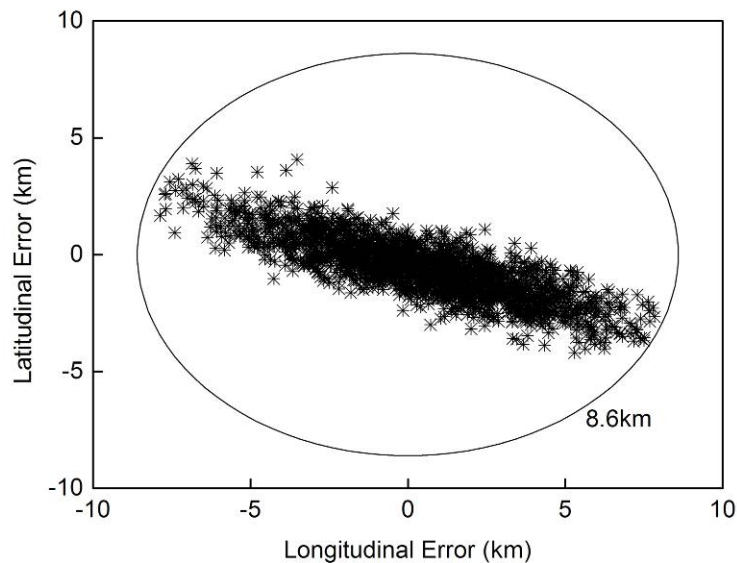
Figure 5. Target Miss Distance Dispersion of EHGO+FL Guidance
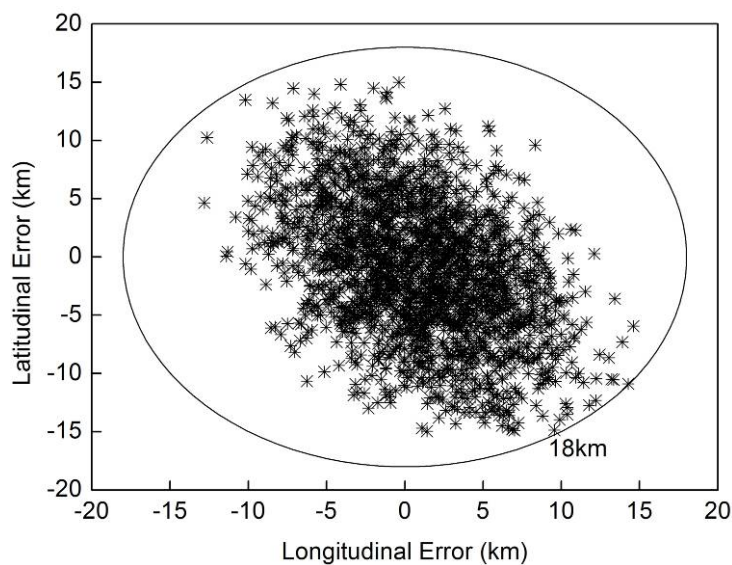
Figure 6. Target Miss Distance Dispersion of FL Guidance

6. Conclusion

To meet the requirement of future Mars exploration, a new drag-based entry guidance method for low lift-to-drag ratio vehicle was present in this paper. An extended high gain observer combined with feedback linearization was applied in drag tracking for Mars entry longitudinal guidance. The FL tracking law and the EHGO+FL tracking law were compared in Mars entry simulations in present of various uncertainties. The results demonstrate that the observer can accurately and enough fast estimate the drag and drag rate. The 2000-run Monte-Carlo simulations show the maximum error corresponding to the worst case for EHGO+FL guidance method is less than 8.6km and is more less than the error for FL guidance method. This validates the robustness and feasibility of the guidance algorithm developed in this article.

References

[1] Steinfeldt BA, Grant MJ, Matz DM, Braun RD. Guidance, Navigation, and Control System Performance Trades for Mars Pinpoint Landing. *Journal of Spacecraft and Rockets.* 2010; 47(1): 188.

[2] Wolf AA, Graves C, Powell R, Johnson W. *Systems for Pinpoint Landing at Mars.* AAS/AIAA 14th Space Flight Mechanics Conference. Maui Hawaii. 2004; 119: 2677-2696.

[3] Saraf A, Leavitt JA, Chen DT, Mease KD. Design and Evaluation of an Acceleration Guidance Algorithm for Entry. *Journal of Spacecraft and Rockets.* 2004; 41(6): 986–996.

[4] Tu KY, Munir MS, Mease KD, Bayard DS. Drag-Based Predictive Tracking Guidance for Mars Precision Landing. *Journal of Guidance, Control and Dynamics.* 2000; 23(4): 620-628.

[5] Talole SE, Benito J, Mease KD. *Sliding Mode Observer for Drag Tracking in Entry Guidance.* AIAA Guidance, Navigation and Control Conference and Exhibit. Hilton Head. 2007.

[6] Hormigo T, Silva JA, Camara F. *Nonlinear Dynamic Inversion-Based Guidance and Control for a Pinpoint Mars Entry.* AIAA Guidance, Navigation and Control Conference and Exhibit. Hawaii. 2008.

[7] Li S, Peng YM. *Neural Networks-based Sliding Mode Variable Structure Control for Mars Entry.* Proceedings of the Institution of Mechanical Engineers, Part G: Journal of Aerospace Engineering. 2011.

[8] Restrepo C, Valasek J. Structured Adaptive Model Inversion Controller for Mars Atmospheric Flight. *Journal of Guidance, Control, and Dynamics.* 2008; 31(4): 937-953.

[9] Alexander IK. Analysis of Predictive Entry Guidance for a Mars Lander under High Model Uncertainties. *Acta Astronautica.* 2011; 68: 121-132.

[10] Benito J, Mease KD. Reachable and Controllable Sets for Planetary Entry and Landing. *Journal of Guidance, Control, and Dynamics.* 2010; 33(3): 641-654.

[11] Harpold JC, Donald E, Gavert. Space Shuttle Entry Guidance Performance Results. *Journal of Guidance, Control, and Dynamics.* 1983; Vol.6(6): 442-447.

[12] Mease KD, Kremer JP. Shuttle Entry Guidance Revisited Using Nonlinear Geometric Methods. *Journal of Guidance, Control, and Dynamics.* 1994; 17(6): 1350–1356.

[13] Khalil HK. Nonlinear Systems, Third Edition*.* New Jersey: Prentice Hall, Upper Saddle River3rd edition. 2002: 420-430.

[14] Freidovich LB, Khalil HK. Performance Recovery of Feedback Linearization Based Designs. *IEEE Transactions on Automatic Control.* 2008; 53(10): 2324-2334.

[15] Kalyana C, Yeng CS. High-gain Observers with Sliding Mode for State and Unknown Input Estimations. *IEEE Transactions on Industrial Electronics.* 2009; 56(9): 3386-3393.